Science of the Total Environment 807 (2022) 150777

Contents lists available at ScienceDirect

Science of the Total Environment

journal homepage: www.elsevier.com/locate/scitotenv

Flood impact on the Spanish Mediterranean coast since 1960 based on the prevailing synoptic patterns

Salvador Gil-Guirado [a,*], Alfredo Pérez-Morales [a], David Pino [b,c], Juan Carlos Peña [d,e], Francisco López Martínez [a]

[a] Department of Geography, University of Murcia and Campus Mare Nostrum (CMN), Campus de la Merced, 30001 Murcia, Spain
[b] Department of Physics, Universitat Politècnica de Catalunya·BarcelonaTech, Esteve Terrades 5, 08860 Castelldefels, Spain
[c] Institut d'Estudis Espacials de Catalunya (IEEC-UPC), Carrer Gran Capità, 2-4, 08034 Barcelona, Spain
[d] Meteorological Service of Catalonia, Carrer de Berlín 38, 08029 Barcelona, Spain
[e] Fluvalps-PaleoRisk Research Group, Department of Geography, University of Barcelona, Montalegre 6, 08001 Barcelona, Spain

HIGHLIGHTS

- We classified thousands of floods with a multivariate method.
- Twelve synoptic patterns explain all flood events at the SMC since 1960.
- We detected an important flood hotspot.
- Positive temporal trends regarding some of the patterns are cause for concern.
- Our results reduce the uncertainty of risk management and decision making.

GRAPHICAL ABSTRACT

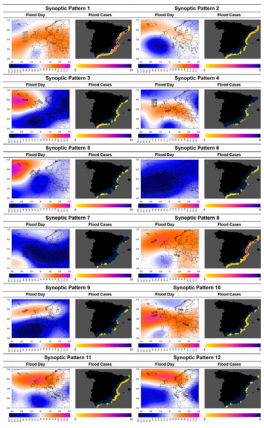

ARTICLE INFO

Article history:
Received 15 July 2021
Received in revised form 29 September 2021
Accepted 30 September 2021
Available online 5 October 2021

Editor: Fernando A.L. Pacheco

Keywords:
Flood hazard
Flood hot spot
20th century reanalysis
Principal component analysis
Synoptic patterns

ABSTRACT

In a changing climate and in social context, tools and databases with high spatiotemporal resolution are needed for increasing the knowledge on the relationship between meteorological events and flood impacts; hence, analysis of high-resolution spatiotemporal databases with detailed information on the frequency, intensity, and impact of floods is necessary. However, the methodological nature of flood databases hinders relating specific flood events to the weather events that cause them; hence, methodologies for classifying flood cases according to the synoptic patterns that generate them are also necessary.

Knowing which synoptic patterns are likely to generate risk situations allows for a probabilistic approach with high spatial resolution regarding the timing of occurrence, affected area, and expected damage from floods. To achieve these objectives, we use the SMC-Flood Database, a high-resolution spatiotemporal flood database covering the 1960–2015 period for all municipalities along the Spanish Mediterranean coast. To relate floods with the synoptic conditions that generated them, we used a multivariate analysis method on the corrected daily anomalies of the surface pressure fields, 850 hPa temperature, and 500 hPa geopotential height, all of which were obtained from the 20th Century Reanalysis Project V2.

Results show that 12 atmospheric synoptic patterns can statistically explain the 3608 flood cases that occurred in the study area between 1960 and 2015. These flood cases were classified into 847 atmospherically induced flood events. These results reduce the uncertainty during decision making because of the classification of potential risk

* Corresponding author.
E-mail address: salvador.gil1@um.es (S. Gil-Guirado).

https://doi.org/10.1016/j.scitotenv.2021.150777

situations. The Mediterranean Basin is a region where floods have serious socioeconomic impacts; hence, this work helps improving prevention measures and providing information for policymakers, mainly regarding land use planning and early warning systems.

1. Introduction

Increasing the knowledge on the relationship between meteorological events and the impact of floods requires high spatiotemporal databases. Analyzing this relationship provides accurate knowledge on the climatic danger of floods, which is an indispensable step toward proper adaptation and prevention regarding dangerous situations. To minimize the loss of human life and reduce the economic consequences of natural disasters, proper planning and risk prevention are essential (Bathrellos et al., 2017).

Regarding the required high-resolution spatiotemporal databases for analyzing the climatic evolution of floods and their effects, there are numerous open-access global-scale flood databases that have been developed in recent years and have increased our knowledge on flood risks at global as well as regional scales (Brakenridge, 2014; CRED. EM-DAT, 2010; Munich Re, 2015; Swiss-Re, 2017). However, the methodological nature of these databases hinder relating local flood events to the synoptic atmospheric conditions that cause them; hence, it is necessary to classify flood cases according to synoptic conditions in order to identify the synoptic patterns that are likely to generate risk situations, as well as their timing and area of influence, both in terms of recurrence probability and probable damage intensity.

Regarding global synoptic meteorological data, the meteorological community has been using real-time forecasts for their analyses only since a few years ago. Owing to great advances in data assimilation systems, this approach produced many heterogeneities in series compiled from synoptic maps, thus causing serious disturbances when interpreting past meteorological conditions. In this context, the National Centers for Environmental Prediction (NCEP) / National Center for Atmospheric Research (NCAR) reanalysis project (Compo et al., 2011; Kalnay et al., 1996) was created to standardize the analysis of synoptic configurations.

The large methodological disparity in data types and the scale at which flood databases are analyzed hinder associating these two types of information sources. In this regard, most studies have focused on the relationship between rainfall and the synoptic atmospheric conditions that cause it (Romero et al., 1999a), thus pushing the causal relationship with flood impacts on the background. The latter relationship is especially important, since geographical conditions and exposure levels of goods and people ensure that not all extreme precipitation events generate floods. In this sense, determining the flood risk is a complex process in which anthropic factors may explain social impacts and consequences (Gil-Guirado et al., 2016), which can change over time (Maddox et al., 1995).

Numerous studies have indirectly linked synoptic patterns with floods by classifying conditions that generate heavy rainfall. Niedźwiedź et al. (2015) identified three types of circulation that are directly related to episodes of intense rainfall in the Tatra Mountains in Poland. Peleg and Morin (2012) examined the spatiotemporal characteristics of convective rain cells in northern Israel and their relationship to synoptic patterns. Similarly, and for the same region, Armon et al. (2018) identified the spatiotemporal characteristics of storms and floods for each circulation pattern. All these studies used reanalysis databases, quantitative rainfall estimates from weather radar, and hydrological data. In this sense, Romero et al. (1999a) conducted a landmark study and identified 11 main synoptic patterns that explain a large part of the variance in extreme rainfall in the Spanish Mediterranean region; they used a database covering 30 years of daily rainfall at 410 locations in the area to derive the main spatial patterns that control significant and torrential daily rainfall.

To summarize, the direct relationship between floods and the synoptic conditions causing them has been studied only marginally. Broadly speaking, there are two types of studies that relate synoptic patterns to the impact and extent of floods: 1) Reconstruction of the synoptic conditions during recent catastrophic floods (Gochis et al., 2015; Kahana et al., 2002; Lira et al., 2013; Lynch and Schumacher, 2014; Milrad et al., 2015), and 2) reconstruction of historical catastrophic floods by using synoptic patterns (Llasat et al., 2005; Pino et al., 2016; Stucki et al., 2012; Trigo et al., 2014). Regarding the first type of studies, some of the authors have reconstructed synoptic patterns for a large number of floods; however, their studies were not systematic, continuous, and homogeneous with a focus on time and space. For example, Kahana et al. (2002) analyzed sea-level pressure, 500 and 250 hPa geopotential heights, 850 hPa temperature, and 500 and 250 hPa wind components, for which they manually classified the synoptic types that caused 52 floods in the Negev Desert in Israel over the 1965–1994 period. The authors considered only floods with a maximum discharge above the magnitude of the 5-year recurrence intervals in at least one drainage basin, and they did not contemplate whether or not these maximum discharges impacted society in any way. Regarding historical floods, Pino et al. (2016) analyzed the synoptic situations of 24 catastrophic floods that generated the greatest social impacts in Catalonia, Spain during the 1842–2000 period; however, this was not a systematic study of all the floods in that region and focused solely on catastrophic floods. Llasat et al. (2005) made an initial approximation of the meteorological patterns related to floods occurring between 1840 and 1870 in the same area by manually classifying 62 floods that were reconstructed based on cultural documentations and, had therefore impacted society when they occurred. However, instrumental atmospheric data from the 19th century allowed only an approximation of the synoptic configurations at the surface. Furthermore, the synoptic classification is subjective, which prevents the extrapolation of the selected methodology. Finally, Stucki et al. (2012) reconstructed the synoptic patterns of 24 catastrophic floods that occurred between 1868 and 1910 in large basins at the central Alps, which were derived from instrumental and documentary rainfall data and 20th Century Reanalysis data (Compo et al., 2011); in that case, catastrophic floods were determined by the 95th percentile of the differences between an annual flood and a defined contemporary flood.

Regarding the methodology, the relationship between synoptic patterns and floods or intense rainfall has generally been analyzed indirectly through manual reconstruction of synoptic patterns and the rainfall patterns that they are likely to generate (Elsner et al., 1989; Kahana et al., 2002; Llasat et al., 2005; Maddox et al., 1979). Although this methodology constitutes a notable development, it is subjective in nature. In Spain, Armengot et al. (1996) used a subjective manual classification method to analyze precipitation patterns of more than 100 mm/d in the Valencian autonomous community (i.e., eastern Spain; 131 cases analyzed). Conversely, Ortega et al. (2018) carried out a subjective classification of synoptic conditions during precipitation episodes of more than 100 mm/day in the autonomous region of Murcia (i.e., southeastern Spain) between 1980 and 2000.

However, advances in computing have ensured that systems for classifying rainfall and synoptic conditions are no longer based on subjective manual procedures, but instead rely on objective or semi-objective automated computing criteria. In this respect, a wide variety

of automated or semi-automated classification methods exists (Huth, 1996a), although the most widely used methods are those based on principal component analysis (PCA) and/or cluster techniques. Romero et al. (1999b) reconstructed the synoptic patterns associated with high intensity rainfall in the Mediterranean region of Spain using PCA and clustering techniques. Similarly, García-Valero et al. (2012) classified clusters and performed an atmospheric circulation PCA over the Iberian Peninsula according to the circulation types obtained from sea-level pressure and the 500 hPa geopotential height between 1958 and 2008; however, they reconstructed all these patterns without considering rainfall or flood data, thereby reducing the potential of their method for assessing the flood risk. Esteban et al. (2006) applied PCA and clustering techniques to characterize daily surface synoptic circulation patterns for western Europe and northern Africa over the 1960–2001 period, for which they used data from the NCEP/NCAR reanalysis project. Martin-Vide et al. (2008) performed an automated classification of synoptic patterns causing torrential rainfall in Catalonia, based on a PCA of 304 days with precipitation ≥100 mm/day during the 1950–2005 period. Finally, Gilabert and Llasat (2018) used the automatic classification system of Jenkinson and Collison to classify the synoptic conditions of 261 extraordinary and catastrophic flood and flash flood events recorded during the 1900–2010 period in northeastern Spain. The authors used newspaper information to assess the ensuing social impacts of the analyzed floods; however, they did not consider all the floods that happened in the area in the 1900–2010 period because they did not consider them to be ordinary floods.

So far, no work has reconstructed the synoptic patterns of a large number of flood cases that have been classified according to their damages to assets and people. This is a major shortcoming in flood risk prevention because, by basing flood warning systems strictly on hydrological and meteorological criteria, any analysis of synoptic conditions that actually inflict harm on society is pushed to the background. Conversely, because the literature directly links flood risk to synoptic conditions, it does not include the least damaging and most severe types of floods, which constitutes a major problem when it comes to forming a complete picture of flood risk in a given region (Cherqui et al., 2015). Since less severe floods are much more frequent than catastrophic floods, and the latter are decreasing due to prevention measures, extraordinary floods are increasing due to increased exposure to flood risk (Barriendos et al., 2019).

In this respect, the main objective of this study is to form a complete view of the synoptic conditions that generate floods that impact society and to analyze their spatiotemporal variability over the last 55 years along the Mediterranean coast of Spain (Fig. 1), i.e., a region of enormous economic and social dynamism. In recent decades, the region has undergone an accelerated transformation in the wake of mass tourism, which is a favorable economic situation that has also led to an excessive increase in population and urban space; however, this whole process has materialized in an environmental scenario that involves great flood risk, which has become the number one natural risk in the region (Pérez-Morales et al., 2018).

To achieve our objectives, we implemented an automated and objective synoptic classification methodology that can be applied in similar study areas. In this study, we adapted the methodology proposed by Romero et al. (1999a, 1999b) by using direct data of flood intensity and frequency along the Spanish Mediterranean coast (SMC) between 1960 and 2015. These data were obtained from the SMC-flood database developed by Gil-Guirado et al. (2019), which includes 3608 flood cases.

Despite the development of new management tools, policymakers currently have limited available information to support their planning and prevent floods (Arrighi et al., 2019). For this reason, by using the proposed methodology, synoptic conditions can be identified based on their potential for damage to the population, as only those that generate some type of damage to the population are considered. In addition, owing to the large number of events examined, our method provides a high level of confidence in analyzing the spatiotemporal variability of the synoptic patterns associated with floods.

In summary, this study performs a multidisciplinary analysis of the interface between the atmosphere, hydrosphere, and anthroposphere, while the methodology combines approaches of both social and environmental sciences. Kourgialas and Karatzas (2017) used a holistic methodology to detect areas prone to flood risk; their results focused on helping flood risk planning, and adaptation. This type of work has added value because it facilitates a holistic quantitative approximation regarding the analysis of the complex dynamic system comprised of the environment and society (Monge et al., 2022).

The remainder of this paper proceeds as follows: Section 2 describes the flood database, the methods for grouping flood cases into precipitation events, and the methodology for classifying the synoptic patterns associated with these events. Section 3 includes the results obtained from analyzing the spatial variability of the impacts relative to the different detected synoptic patterns, while a trend analysis relates spatiotemporal variability to changes in natural flood hazards. Discussion is presented in section 4. Finally, in Section 5, we summarize the main conclusions of the study.

2. Data and methodology

Two different databases (i.e., flood cases and meteorological data) were combined to reconstruct the most common synoptic patterns causing floods in the study area. The considered floods were obtained from the SMC-flood database developed by Gil-Guirado et al. (2019);

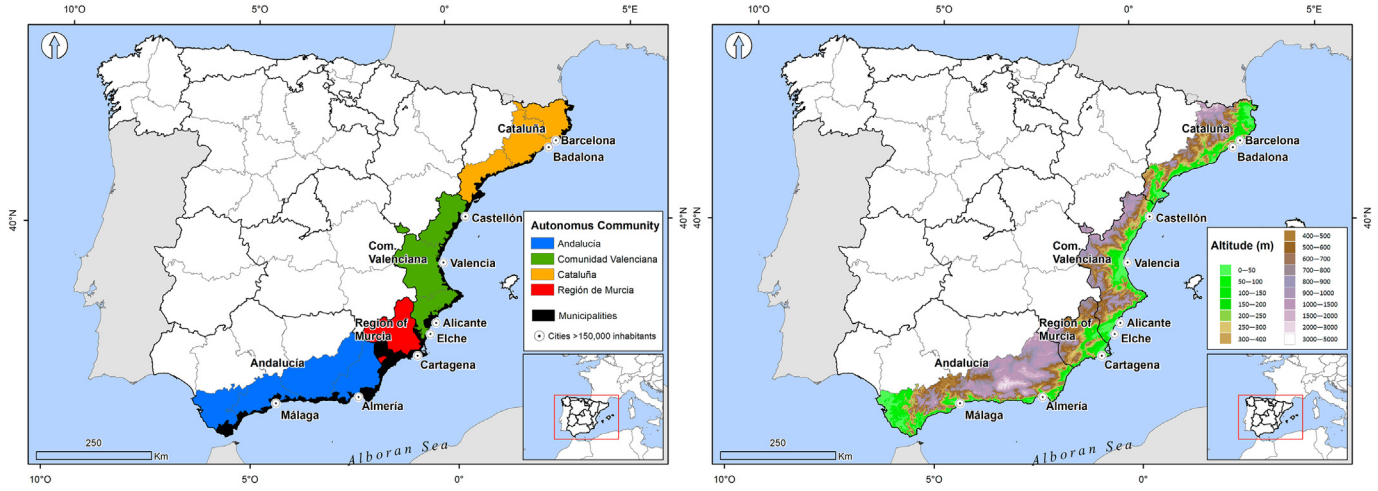

Fig. 1. Map of the Spanish Mediterranean coast. (Left) SMC provinces, autonomous communities, and cities with more than 150,000 inhabitants; (Right) relief of the coastal provinces.

this database contains information on floods that occurred in municipalities along the Spanish Mediterranean coast between 1960 and 2015 and was reported by newspapers. Thus, our primary sources of information are the newspaper archives of the most widely circulated newspapers in each of the four autonomous communities studied that were continuously published during the study period. We searched for flood events in the newspaper archives by interrelating a series of keywords and the name of each municipality along the SMC (in total 179 municipalities). The keywords correspond to the most common ways of referring to a situation that is likely to describe a flood in Spain: "inundación" (flood); "inundaciones" (floods); "riada" (flash flood); "lluvias torrenciales" (torrential rains); "fuertes lluvias" (heavy rains); "intensas lluvias" (intense rain); and "tromba de agua" (severe downpour).

All floods mentioned in the newspapers were related to affected municipalities and flood dates. Each flood case was classified according to its level of intensity based on the following three levels (Barriendos et al., 2019; Gil-Guirado et al., 2019; Llasat et al., 2005): Level 1 (L1) is an ordinary flood, a flood without overflow that incurs minor damage. Level 2 (L2) is an extraordinary flood, a flood with overflow that incurs major damage. Level 3 (L3) is a catastrophic flood, a flood with overflow that causes general destruction, and deaths. Additionally, the SMC-flood database classifies the type of damage in each case through 10 dichotomous variables that indicate the presence (1) or absence (0) of any of the following effects/damages produced by the flood in each municipality: agriculture, cattle, fishing, road and urban furniture, industry, trade, houses and buildings, tourism, injured people, and fatalities. To present the results of this study, we grouped these dichotomous variables into three common economic sectors. In this way, we followed the classic classification of economic sectors and considered the primary sector to be the economic sector where damage is incurred on agriculture, cattle, and fishing; the secondary sector is where damage is incurred on industry; and the tertiary sector is where damage is incurred on trade and tourism.

For the meteorological database, we used the 20th Century Reanalysis data at 2.5° resolution (Compo et al., 2011) to classify the synoptic configuration in each flood day (KD) plus the six previous days in order to analyze the evolution of the meteorological conditions prior to the flood. The gridded area spanned from 30°N to 70°N and from 30°W to 30°E. The variables chosen in this study were sea level pressure (SLP), 850 hPa temperature (T850), and 500 hPa geopotential height (Z500). We used normalized anomalies of variables corrected by the square root of the cosine of latitude (in radians), which was required to account for the convergence of the meridians (i.e., area weighting), thereby lessening the impact of high-latitude grid points that represent a relatively smaller area of the globe.

The methodology for combining the flood and meteorological databases was carried out in four steps. In the first step, we classified the 3608 cases (where one case is equivalent to a municipality affected by a flood on a specific date) into 1088 flood events occurring on different days.

In the second step, we grouped these flood events according to their synoptic patterns. To analyze the synoptic conditions corresponding to the flood events, the method we used was a multivariate analysis of the corrected daily anomalies of SLP, T850, and Z500. This methodology has been applied by earlier studies and proven viable for studying the synoptic patterns producing hail (Aran et al., 2011) and strong winds in Catalonia (Peña et al., 2011), as well as the excess mortality due to heat waves in Barcelona (Peña et al., 2015). As Huth et al. (2008) indicated, PCA has a two-fold utility regarding the classification of synoptic patterns: It can be applied in S-mode as a tool prior to cluster analysis (CA) or in T-mode as a classification tool. In this study, we used PCA prior to CA, and thus it cannot be considered as a classification tool because the posterior CA served as such.

PCA was used only as an intermediate tool for data dimension reduction, i.e., a procedure that we applied individually to every third dataset using an S-mode data matrix, meaning that the variables were grid points and the observations were days. We also used a correlation matrix, for which we employed the Scree test as criterion for determining the number of components involved, i.e., we would stop including components in the analysis after detecting a change in the slope of the sedimentation graph (Cattell, 1966; Huth, 1996b). To rotate the components that minimize the number of variables with high factor loadings, we used the orthogonal varimax procedure, which reduces the dependence among components and satisfies the orthogonality condition of the model (Richman, 1986).

CA was applied to the factor-score matrix, which comprised three individual factor-score matrices obtained through the PCA. The non-hierarchical K-means method served as our clustering algorithm, for which the number of groups to be obtained must be defined beforehand. Although different sophisticated techniques have been developed by other authors (e.g., Debatty et al., 2014; Tibshirani et al., 2001), the choice of number of clusters is still quite subjective. Different parameters can be used to determine the number of initial clusters, such as the variance explained by clusters against the number of clusters, or the minimized total within-cluster sum of squares (WSS) (Thorndike, 1953; Aran et al., 2011; Zhang et al., 2016). The latter is the parameter used in this study, while the 'elbow method' was applied to the hierarchical Ward cluster (which does not need the initial number of clusters) to define the number of clusters such that the total WSS is minimized: first, the WWS for each cluster was calculated; second, the curve of WSS was plotted according to the number of clusters; and third, the location of a bend (knee) in the plot was taken as an indicator of the appropriate number of clusters. This was the initial number of clusters for K-means, which was applied to obtain the groups (Aran et al., 2011; Peña et al., 2011).

In the third step, discriminant analysis (DA) was applied to validate the model and reclassify the borderline events if necessary (e.g., Michailidou et al., 2009). The DA needs predefined classes to classify the cases (e.g., Sioutas and Flocas, 2003), for which manual classification is usually used in this type of analysis. For this step, we used the initial classification obtained from the CA. The factor scores were used as predictors for discriminant analysis, i.e., each day of the factor-score matrix had a group assigned by the CA, while a stepwise selection criterion known as the Wilks' lambda criterion was applied to obtain the discriminant functions (Diab et al., 1991).

Finally, after we synoptically classified the 1088 flood events, we reduced them to a smaller number of flood events (847), because those that occurred on consecutive days under the influence of the same synoptic pattern were in fact the same event. Therefore, we defined a flood event as a day or time period in which a synoptic pattern produced intense rainfall, thereby triggering floods that may have affected one or more municipalities.

In this respect, there was a clear difference between flood cases and flood events. While a flood case refers to a municipality affected by flood on a specific day, a flood event refers to a specific atmospheric situation that could cause one or several flood cases and last for one or several days (Gil-Guirado et al., 2019).

To show the differences in flood incidences according to each identified synoptic pattern, we conducted spatiotemporal analysis. By incidence, we mean the number of flood cases or flood events per spatial unit (i.e., municipality or province) or time (i.e., season or year). Spatial variability was analyzed using cartographic analysis, which revealed hotspots of special incidences in each pattern. Regarding temporal variability, we analyzed both the seasonal and annual variabilities. For seasonal variability, we analyzed the differences in incidence, intensity, and type of damage in each synoptic pattern for each month and season of the year.

Finally, to determine whether temporary changes exist regarding the incidence and intensity of each pattern over the study period, we conducted a trend analysis, for which we used the non-parametric Mann-Kendall test modified by Hirsch and Slack (1984) to identify

any possible trends in the series. From a statistical point of view, the data were considered to present a trend when the *p*-value of the Mann-Kendall test was less than 0.05. This method is widely used in hydrological and climatic studies (Kisi and Ay, 2014). Additionally, we calculated Sen's slope (Sen, 1968) to determine the slope and, therefore, determine the magnitude of the trend detected per unit of time. In other words, with the data used in this study, Sen's slope reported the annual increase or decrease in intensity, number of cases, and number of events for each pattern between 1960 and 2015. The sum of the slopes indicated the total change throughout the study period.

Cartography was conducted using the open-source QGIS software (QGIS Development Team, 2016); trend analysis and slope calculations were performed using the R software (R Core Team, 2019) and the trend support package developed by Pohlert (2016).

3. Results

The methodological procedure described above produced two main results. First, 847 different flood events were distinguished from the 3608 flood cases that occurred along the SMC. Second, we identified 12 main synoptic patterns capable of generating floods. Table 1 presents the results of the main characteristics of the signal patterns. Two synoptic patterns (i.e., PSP1 and PSP8) were responsible for 59% of the flood events. Regarding seasonality, 80% of the flood events occurred mainly during autumn, although a minority of winter synoptic patterns resulted in up to 16% of the flood events. These winter synoptic patterns affected predominantly the central and southern regions of the study area, while the autumn synoptic patterns affected the entire study area, although they occurred mainly in the central and northeastern regions of the SMC. Easterly winds predominated during these events.

3.1. Seasonal differences

The results obtained allowed us to highlight the importance of each synoptic pattern and relate it to the number of flood cases, events, and intensity for each season of the year (see Figs. 2 and 3). Autumn clearly predominated regarding the numbers of both flood events and cases, as well as flood intensity and extent. Besides autumn, winter had the highest number of flood events. In any case, the 12 statistically identified synoptic patterns were grouped into two types of synoptic scenarios.

The first synoptic scenario included PSP5, PSP6, PSP7, and PSP12, all of which were more common during winter and had very low incidence (i.e., less than 13% of flood events and 8% of flood cases related to these four grouped synoptic patterns).

The other synoptic patterns presented similar configurations and higher incidence along the SMC. Flood cases and events associated with these synoptic patterns were distributed across all months of the year; nevertheless, these flood events were clearly predominant during autumn (September –November). This type of weather causes precipitation in the territory when the zonal index is low.

From a spatial point of view, the synoptic patterns exhibited notably different spatial incidence depending on the season (Fig. 4). Despite the fact that PSP1 was more frequent in equinoctial seasons, its incidence during winter was so relevant that it even occupied the first position among the synoptic patterns that caused floods in winter. PSP1 was followed by PSP3, PSP8, and PSP6; however, while PSP1 and PSP8 were distributed across all the SMC municipalities, PSP3 and PSP6 had their winter flood cases concentrated in the southwestern SMC municipalities. In this regard, municipalities located west of the city of Málaga constitute a hot spot where winter flooding has been very frequent. Other secondary winter flooding hot spots were the city of Málaga and the coastal stretch between the cities of Castellón and Murcia.

Results were notably different regarding spring flooding, when PSP8 concentrated the most flood cases, followed by the rest of the synoptic patterns. The most important spring flooding hot spot corresponded to the coastal stretch between the cities of Valencia and Alicante.

In summer, more than 75% of the cases were concentrated in PSP8 and PSP1. Most of the summer floods were concentrated in the municipalities east of the SMC, with almost no flood occurrence in the municipalities located west of the city of Almeria. The city of Barcelona and its metropolitan area constituted summer flooding hot spots; the coastal stretch between the cities of Valencia and Alicante constituted a secondary summer hot spot.

Finally, in autumn, nearly the entire SMC was a large hot spot for floods; however, in the detected areas, autumn flooding was constant and occurred biennially. Again, PSP1 and PSP8 presented a greater number of flood cases and marked effects along the SMC. Other secondary patterns (i.e., PSP2, PSP10, and PSP11) also presented significant autumn recurrences. Spatially, two important autumn flooding hot spots were detected: Barcelona and its metropolitan area, as a result of the large number of flood cases associated with PSP1, PSP2, and PSP8, and the coast between the cities of Valencia and Alicante, due to the high recurrence of PSP1, PSP3, PSP8, PSP10, and PSP11.

Table 1
Synoptic pattern records summary.

Synoptic pattern	Events and % (N: 847)	Surface low-pressure location	Surface high-pressure location	500-mb through	500-mb ridge	Prevailing wind direction on the SMC	Seasonality	Main affected areas on the SMC
PSP1	290 (34%)	Iceland	Central Atlantic	North Africa/ Iceland	North Sea/ Central Atlantic	W	End of the Summer/Autumn	NE & central
PSP2	83 (10%)	Spanish Atlantic coast		Spanish Atlantic coast	Iceland	S	Autumn	NE & S
PSP3	41 (5%)	Iberian Peninsula	North Atlantic	Iberian Peninsula	North Atlantic	NE	Winter	SE & S
PSP4	12 (1%)	Iceland	Western Europe	North Africa/ Iceland	Western Europe	E	Winter	Central
PSP5	32 (4%)	Western Europe	Iceland	Western Europe	Iceland	NE	All year	NE & SE
PSP6	38 (5%)	North Atlantic		North Atlantic		SE	Winter	S
PSP7	11 (1%)	Iceland/ Central Mediterranean		North Atlantic to Central Europe	Azores isles	S	Winter	S & NE
PSP8	222 (26%)	South Iberian Peninsula	Azores isles	Iberian Peninsula	Azores isles	E	Autumn	Central & NE
PSP9	25 (3%)	SW Iberian Peninsula	N British Islands	SW Iberian Peninsula	N British Islands	SE	Winter	All
PSP10	41 (5%)	N Africa/ Norwegian Sea	N Atlantic	N Africa/ Norwegian Sea	N Atlantic	E	Autumn	Central
PSP11	39 (5%)	North Africa	North Sea	North Africa	North Sea	E	Spring & Autumn	Central & NE
PSP12	13 (2%)	Central Atlantic Ocean	Norwegian Sea	Central Atlantic Ocean	Norwegian Sea	S	Winter	Central & S

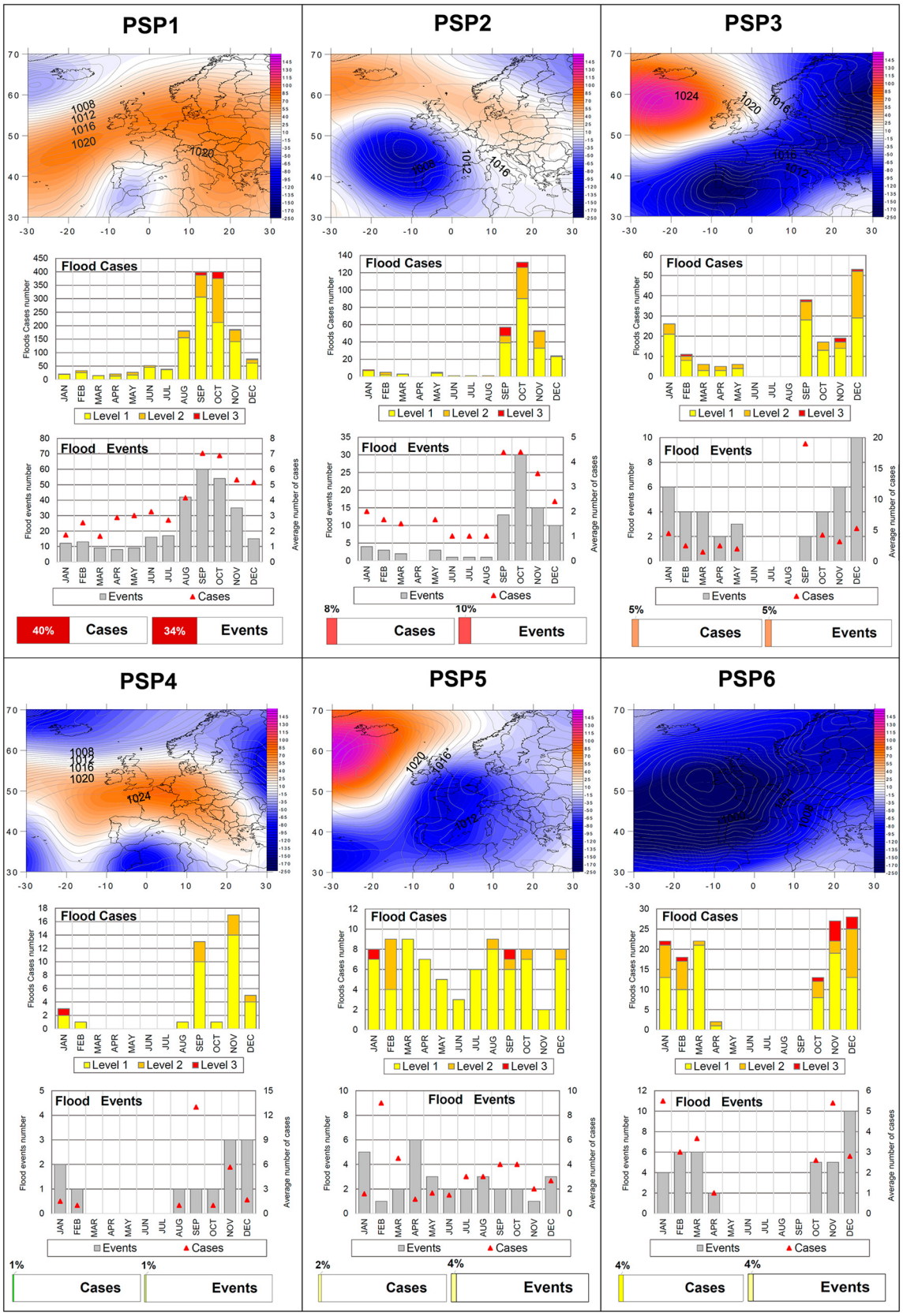

Fig. 2. Seasonal variability of the PSP1–PSP6 synoptic patterns. For each synoptic pattern, the map shows the dominant synoptic conditions on the day of the flood. The upper graph in each synoptic pattern reports the total number of that pattern's flood cases according to month and flood intensity. The central graph reports the total number of flood events per month and average number of municipalities affected (i.e., flood cases) by each flood event and in each month. The lower graph reports the percentage of that synoptic pattern's flood cases and events with respect to the total number of flood cases and events.

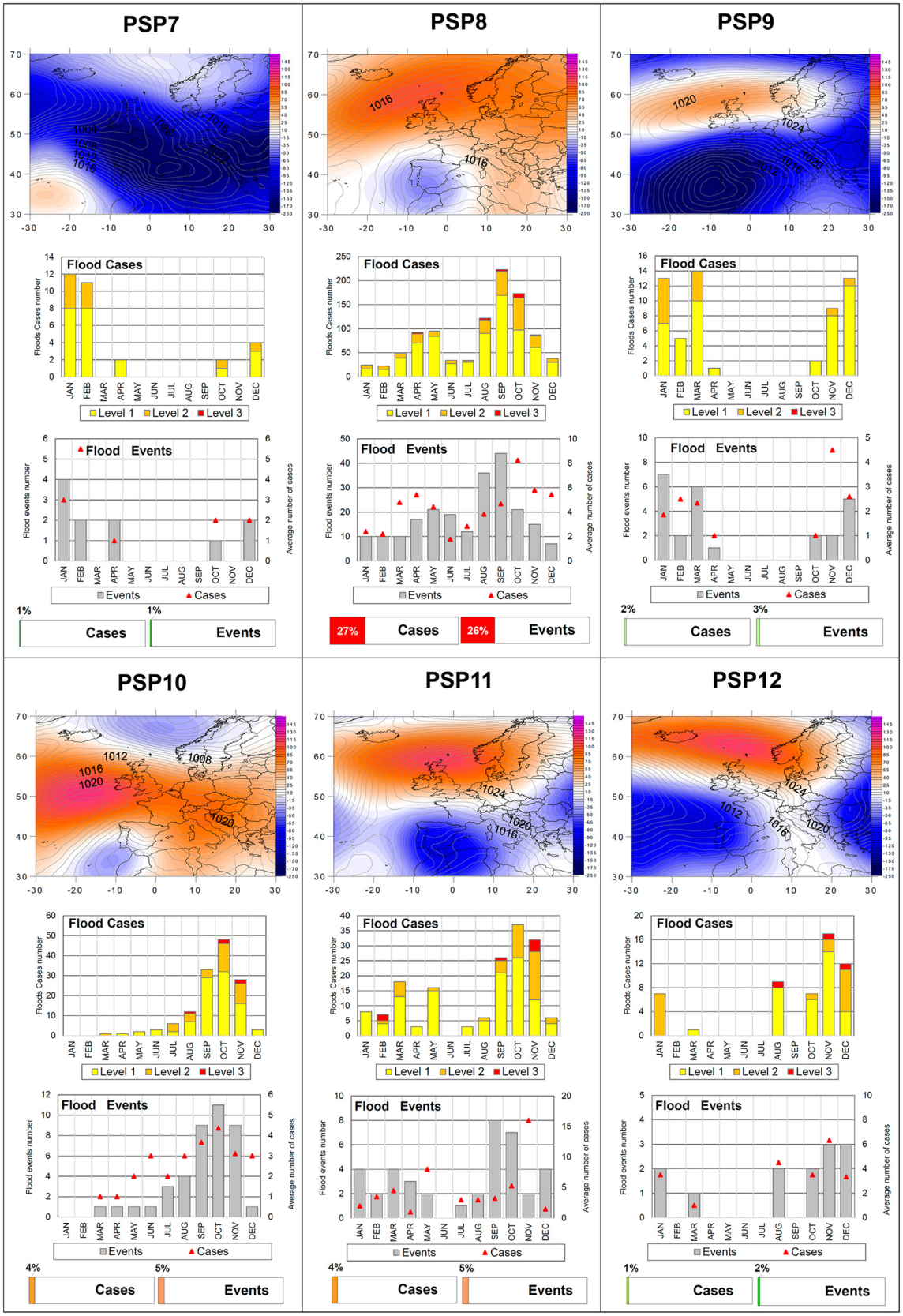

Fig. 3. Same as in Fig. 2, but for the PSP7–PSP12 synoptic patterns.

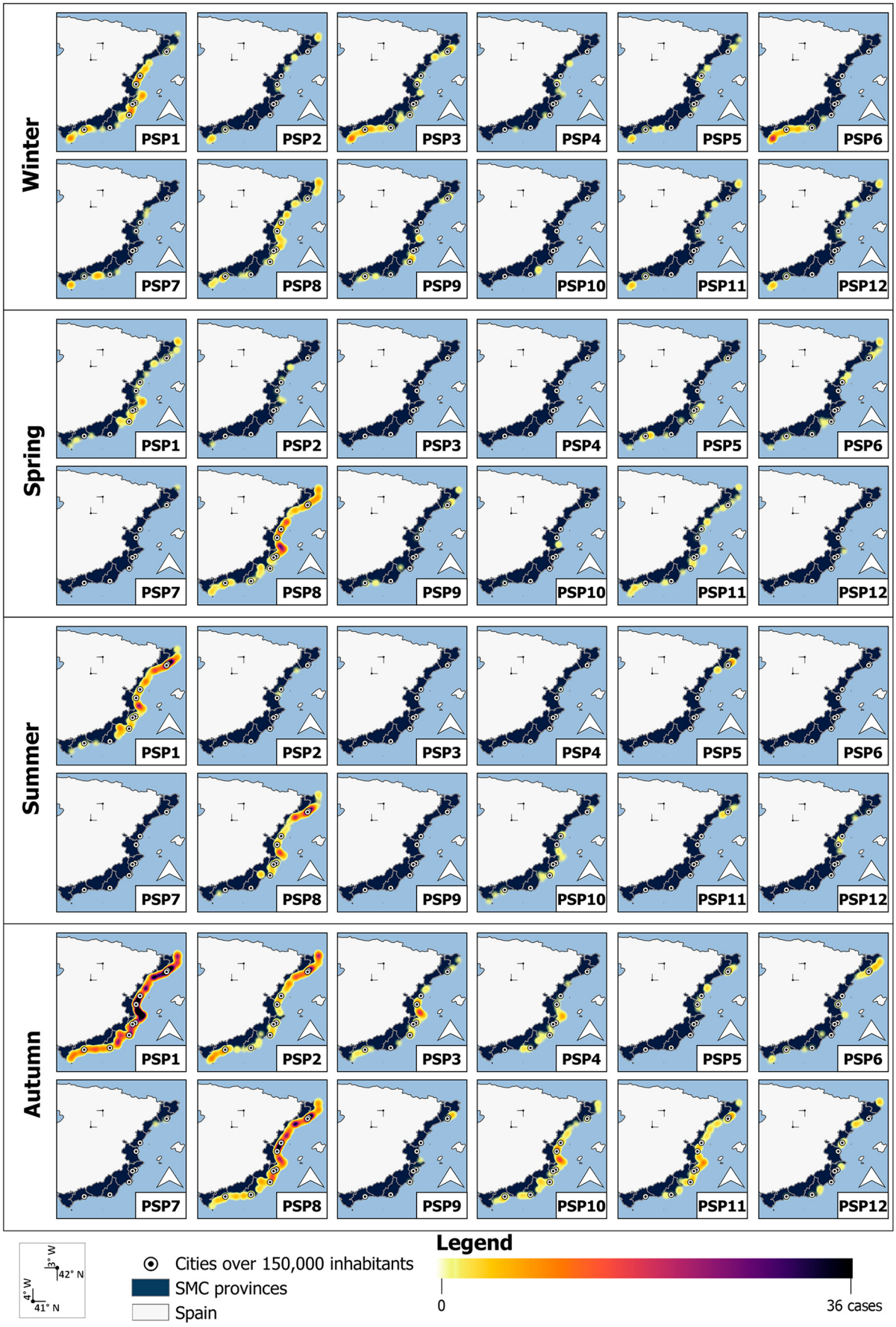
Winter
Spring
Summer
Autumn
PSP1
PSP2
PSP3
PSP4
PSP5
PSP6
PSP7
PSP8
PSP9
PSP10
PSP11
PSP12
3° W
42° N
4° W
41° N
Cities over 150,000 inhabitants
SMC provinces
Spain
Legend
0
36 cases

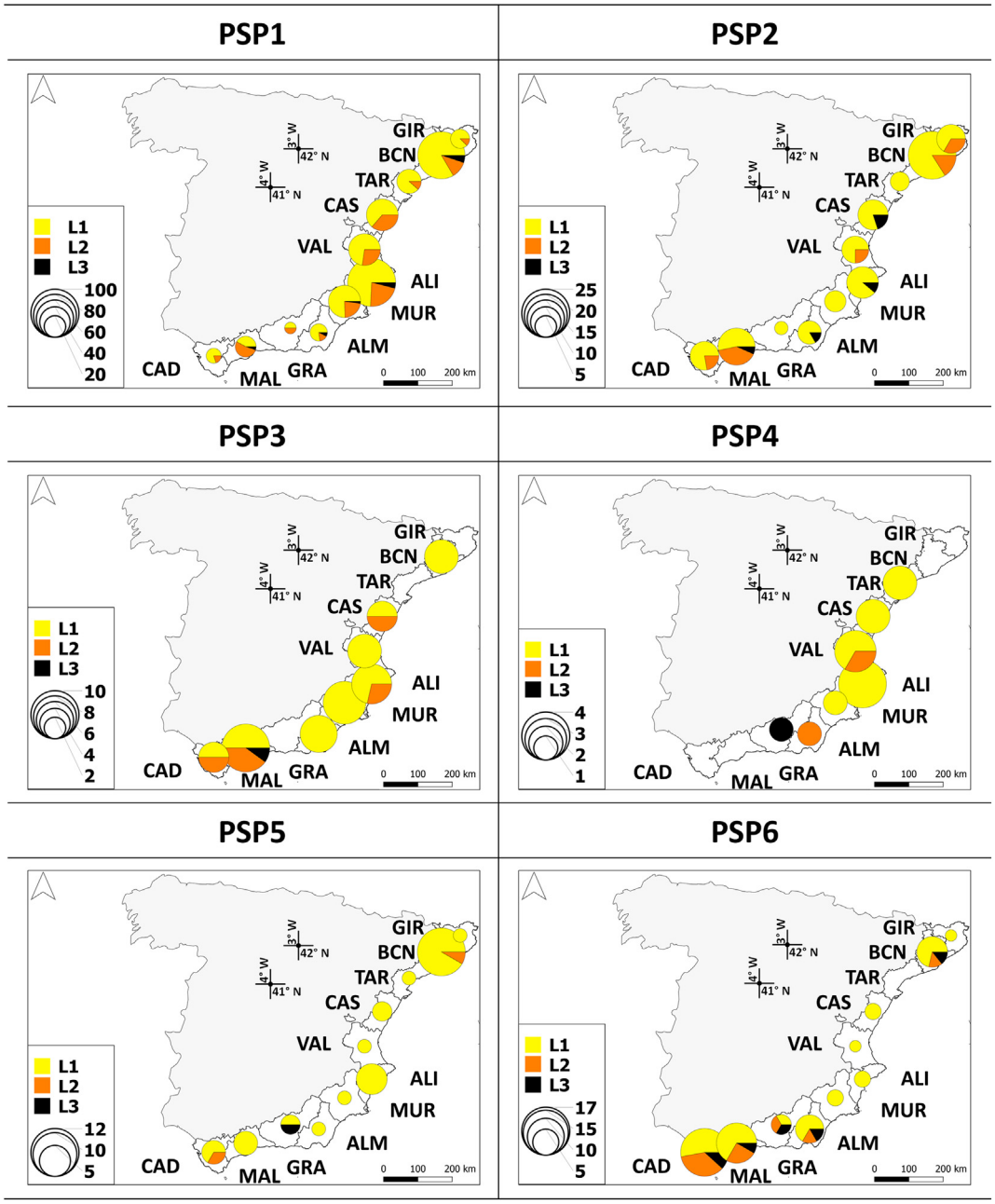

Fig. 5. Spatial variability of flood cases according to flood amount and intensity for the PSP1–PSP6 synoptic patterns. (For better visualization, values are aggregated at provincial level, while legend circles depict the maximum flood-case number of each synoptic pattern at provincial level). Province names are coded as follows: GIR: Girona; BCN: Barcelona; TAR: Tarragona; CAS: Castellón; VAL: Valencia; ALI: Alicante; MUR: Murcia; ALM: Almería; GRA: Granada; MAL: Málaga; and CAD: Cádiz. The legend's value differences among the different synoptic patterns determine the incidence differences in each synoptic pattern.

3.2. Spatial distribution of the synoptic patterns according to their frequency and intensity

The areas with the highest flood incidence were the southeastern and northeastern SMC; however, there were notable spatial differences depending on the synoptic patterns (see Figs. 5 and 6). PSP1 had high incidence across the entire SMC, especially the central and northeastern areas, and smaller impact on the southwestern area. This synoptic pattern had the greatest accumulated incidence in the provinces of Alicante and Barcelona. With regard to the severity (i.e., level 1, 2, and 3 flood-event percentages), PSP1 produced more intense floods in the provinces of Valencia and Murcia, with significant level 2 and 3 flood-event percentages. PSP2 had moderate incidence across the SMC and a homogeneous impact; however, the northeastern and southwestern areas stood out in terms of number of flood events. In the central and southwestern areas, the impact of PSP2 had greater intensity, which was also the case for PSP3 in the southwest area. In the latter case, the general incidence was low and focused on the central and southern areas. PSP4 had very

Fig. 4. Flood cases at municipal level according to synoptic pattern and season. Cities with more than 150,000 inhabitants along the SMC are (from north to south): Badalona, Barcelona, Castellon, Valencia, Alicante, Elche, Cartagena, Almeria, and Málaga.

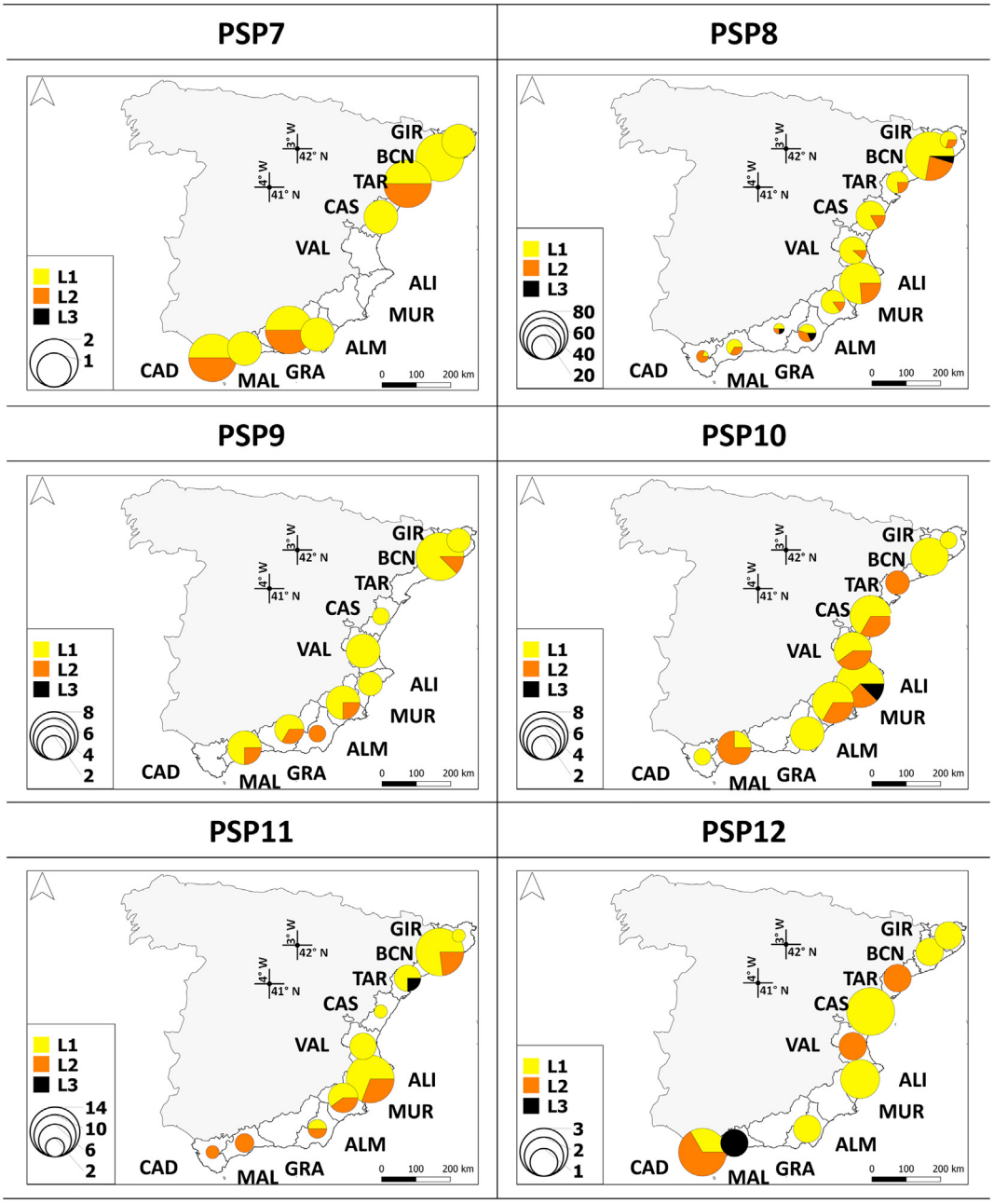

Fig. 6. Same as Fig. 5, but for the PSP7–PSP12 synoptic patterns.

low incidence, which was focused on the central and southeastern areas. The highest severity of this synoptic pattern occurred in the provinces of Almeria and Malaga; however, in these provinces, PSP4 generated only one flood, i.e., the differences in intensity were not significant. Conversely, PSP5, PSP6, PSP7, and, to a lesser extent PSP12, were similar to PSP2 as they exhibited a southwest–northeast dipole corresponding to a higher incidence and severity of flood events. This dipole is a consequence of the dominant synoptic Mediterranean (i.e., PSP5) or Atlantic (i.e., PSP6) low-pressure center, or a mixture of both (i.e., PSP2, PSP7, and PSP12). In these cases, the Atlantic low generally affected the southwestern municipalities first, while it intensified over the Mediterranean Sea, where it affected the northeastern municipalities (Table 1).

PSP8 had high general incidence that concentrated especially on the eastern SMC. The severity of flood cases associated with this synoptic pattern was higher in the southern SMC. PSP9, PSP10, and PSP11 had low incidences and affected the entire study area. PSP10 stood out for its high flood severity and concentration of large numbers of flood events in the central and southeastern areas.

Generally speaking, the synoptic patterns of higher spatial flood incidence (i.e., PSP1 and PSP8) as well as other secondary synoptic patterns, exhibit spatial coherence and higher flood incidence and intensity between the provinces of Alicante and Girona. These two synoptic patterns show similar synoptic configurations, i.e., low-pressure areas over the Mediterranean Sea and east or northeast surface fluxes, which together induce a warm and moist flux over the Girona, Barcelona, and Alicante provinces (Table 1).

3.3. Relationship between synoptic patterns and flood damage

Panel A of Fig. 7 shows for each month of the year the percentages of flood events that caused damage, according to type and the economic sector affected, panel B of Fig. 7 shows, the same types of percentages, but for each synoptic pattern.

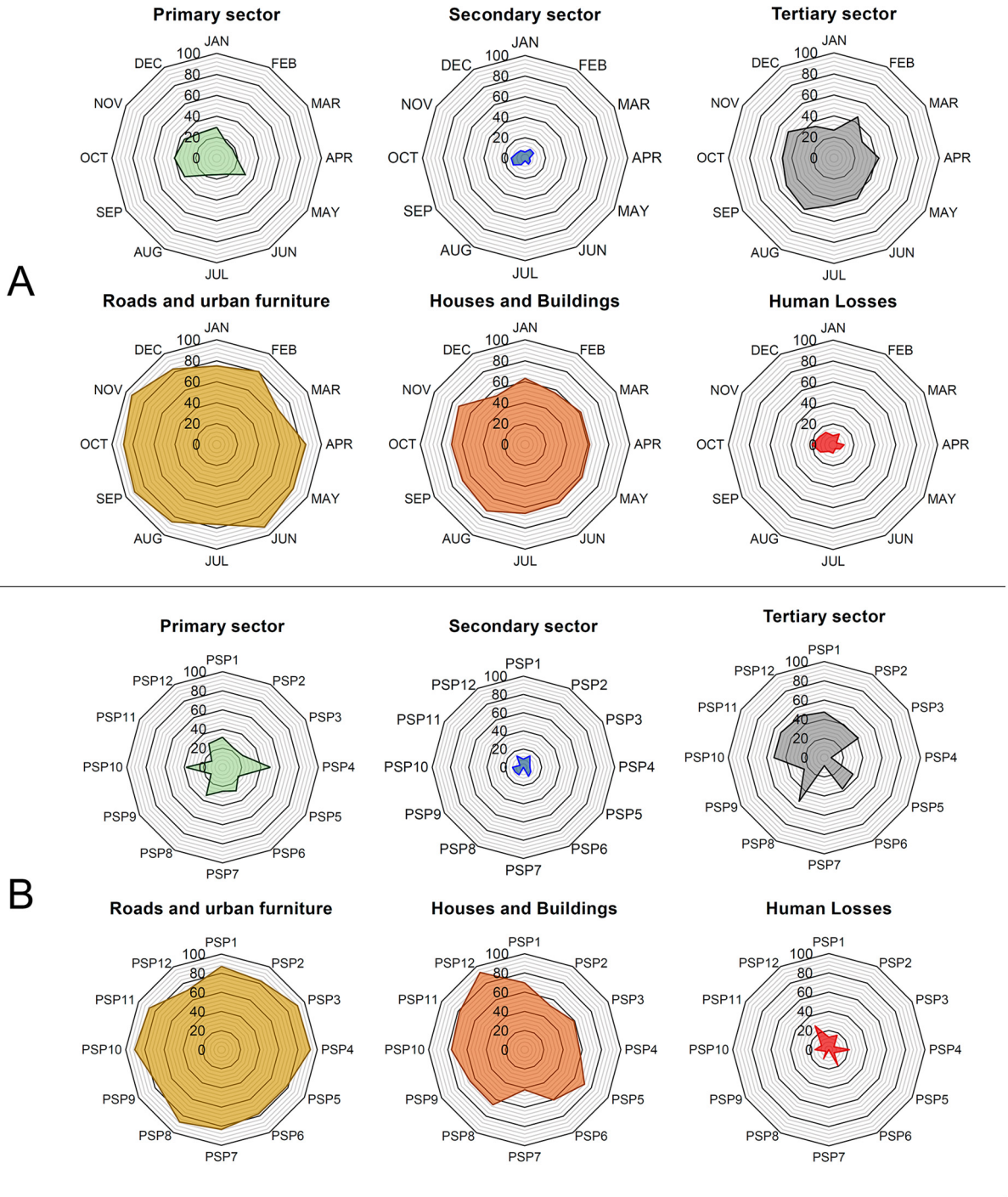

Fig. 7. Distribution of the type of flood damage by month (panel A) and pattern (panel B).

Looking at damage by economic sector, the tertiary sector of the SMC was the most affected by floods, followed by the primary and secondary sectors; trade was impacted the most. We note that most commercial establishments are located at the ground floors of buildings and are therefore prone to flooding in the event of overflowing waters; however, damage to the primary sector was related to the flooding of crop fields. In the study area, the most dangerous months for the tertiary sector were from August to November, during which almost 40% of the flood events caused damage to commerce and tourism.

Regarding the type of damage, it is important to note that almost 80% of flood events produced damage to roads and urban furniture. Damage to roads resulting from flooding or road breakage during floods is especially important. Damage to houses and buildings was also widespread, as more than 60% of flood events impacted these structures. Finally, less than 20% of flood events resulted in human losses.

At monthly level, it was again the autumn months and end of summer when the greatest flood impact occurred in terms of all types of damage. Noteworthy was the monthly variability in human losses, since mitigation of this flood impact is where the greatest efforts should be concentrated. In this regard, 20% of the floods that occurred in October incurred human losses, followed by November (15%), and then September and December (almost 14% in both months).

For each synoptic pattern (Fig. 7, Panel B), varying degrees of danger were detected according to the sector and type of damage. In general, PSP10 and PSP12 produced more damage in absolute terms, followed by PSP1 and PSP8, which are especially alarming since almost two-thirds of all flood events were concentrated in these two patterns. We note that, of the 13 flood events that affected more than 25 municipalities, only two were not caused by PSP1 or PSP8.

Regarding damage by sector, the most dangerous synoptic patterns for the primary sector were PSP4, PSP10, and PSP8 (i.e., 50% of these synoptic patterns' flood events damaged the primary sector). The secondary sector was more sensitive to PSP2 and PSP12. The tertiary sector was especially vulnerable to PSP8 and PSP10 (i.e., 52% of flood events in each of these patterns damaged the tertiary sector).

For roads and urban furniture, and houses and buildings, all flood events had high level of danger, with impact values above 60% for almost all synoptic patterns; however, PSP3 and PSP4 were particularly pernicious for roads and urban furniture, whereas houses and buildings were impacted more by PSP12 in 93% of its flood events. Finally, PSP12 requires special attention, as almost one in three floods associated with this synoptic pattern caused human losses.

3.4. Trend analysis

Trend analysis revealed statistically significant temporary changes in the behavior of each pattern. In this regard, some important facts need to be highlighted: First, we detected an annual decrease in average intensity of flooding events; however, the two synoptic patterns that generated increasingly intense flood events were PSP3 and PSP11, which had high incidence in the provinces of Alicante and Murcia and caused a great amount of damage in the tertiary sector. Second, four synoptic patterns (i.e., PSP1, PSP3, PSP8, and PSP11) exhibited increasing numbers of flooding cases during the study period. Flood events associated with these synoptic patterns affected an increasing number of municipalities each year. This increase is especially relevant since it affected the synoptic patterns of greatest recurrence (i.e., PSP1 and PSP8), which in turn led to increased annual average total number of flood cases per flood event. PSP1 and PSP8 exhibited the most increased annual average numbers of flood cases per flood event, i.e., increased by approximately 30 and 20, respectively. These two synoptic patterns had special autumn incidences and affected particularly the provinces between Murcia and Gerona. In this regard, local emergency planning should consider the fact that flood events affected an increasing number of municipalities and that these relatively larger events tended to be even more concentrated in autumn. Third, three synoptic patterns (i.e., PSP1, PSP3, and PSP11) exhibited increased annual numbers of flood events. PSP1, i.e., the pattern with the highest recurrence, exhibited again the highest rates of change, as the number of associated flood events increased by more than six events over the study period, thereby impacting the fact that the number of flood events is increasing (Table 2).

Table 2
Trends in flood events, cases, and intensity according to synoptic patterns.

	Kendall Tau	Mann-Kendall trend test p-value	Annual Sen's slope	∑ Sen's slope
Annual average intensity				
PSP3	0.2278	0.0267	0.0141	0.7896
PSP11	0.2516	0.0152	0.0114	0.6384
∑	-0.2968	0.0013	-0.0038	-0.2110
Number of cases per year				
PSP1	0.3283	0.0004	0.5333	29.8667
PSP3	0.2766	0.0063	0.1097	6.1432
PSP8	0.2944	0.0016	0.3515	19.6824
PSP11	0.2849	0.0049	0.0805	4.5080
∑	0.3669	< 0.0001	1.5000	84.0000
Number of events per year				
PSP1	0.41950	< 0.0001	0.1076	6.0270
PSP3	0.30595	0.0038	0.0244	1.3664
PSP11	0.32656	0.0018	0.0209	1.1704
∑	0.35606	0.0001	0.2436	13.6401

Note: Trend values were calculated from annual average values (i.e., 1960–2015; $N = 56$). Only synoptic patterns with statistically significant trends (i.e., $p < 0.05$) are shown. The Sen slope (Sen, 1968) calculation indicates the trend magnitude per time unit. The annual Sen's slope reports the annual increase or decrease in flood intensity, number of flood cases, and number of flood events for each synoptic pattern between 1960 and 2015. ∑ Sen's slope is the sum of the annual Sen's slope and expresses the total change over the study period (i.e., 1960–2015). The annual average intensity is the average intensity of all events occurring in a specific year and for a specific synoptic pattern (this value can vary between 1 and 3). The number of flood cases per year refers to the total number of flood cases generated by a particular synoptic pattern in a particular year. The number of flood events per year refers to that of a particular synoptic pattern in a particular year.

4. Discussion

4.1. Synoptic characterization and flood-hazard anticipation

Stationary or slow-moving synoptic and mesoscale systems are responsible for frequent heavy rainfall severely affecting catchments in the western Mediterranean basin (Fiori et al., 2017). However, several studies have highlighted important spatiotemporal differences in the flood magnitude generation and development related to specific characteristics of the synoptic-scale forcing, topography, and soil-moisture preconditioning (e.g.,Giannaros et al., 2020). Torrential rainfall episodes in the SMC can be compared with those analyzed by other authors.

There are evident similarities in the seasonal distribution of episodes between the western and eastern Mediterranean; however, floods in the western Mediterranean occur mainly in autumn and also in winter (e.g., Grimalt-Gelabert et al., 2021), while floods in the eastern Mediterranean are more frequent both at the end of autumn and winter (Giannaros et al., 2020).

Patterns shown in this study are similar to those presented by Martin-Vide et al. (2021), who analyzed the weather types associated with torrential precipitation affecting the provinces of Alicante and Murcia in the period 1941-2017. Days with low pressure from the Atlantic predominate in the southwestern SMC, where isolated low-pressure configurations also predominate.

Central and eastern Mediterranean are affected more by western perturbations (Giannaros et al., 2020). This was highlighted by Seager et al. (2020), who showed that the fraction of variance of mean precipitation during the cold part of the year, explained by the principal North Atlantic Oscillation (NAO) and the principal mode of atmospheric variability in Europe (Hurrell, 1995), varies between less than 10% in the SMC region and around 40% in Italy and the eastern Mediterranean, especially in the Adriatic area. This is related to the meridional shift of the storm tracks, especially in winter and can also explain the slight differences in seasonal distribution of flood events.

In the SMC, the winter synoptic patterns present a North Atlantic low-pressure area centered over the British islands, while the Azores anticyclone is located south of the 35th parallel. Consequently, Spain is between both centers of action and is subject to intense zonal flow from west to east. When these fronts are driven by pronounced deep depressions, they can reach the shoreline and produce heavy rainfall; however, Atlantic storms rarely cause heavy downpours in the Mediterranean. This is due to a series of causes, primarily the leeward position of the westerlies and the Foehn effect emanating from the inland mountainous reliefs of the Iberian Peninsula.

Autumn synoptic patterns were the most frequent. These synoptic patterns occur when the low-pressure centers from North Africa install themselves in the Alboran Sea or in the Algerian Maghreb, such that the cyclonic circulation sends winds from the southeast and east to the coast, where the coastal relief forces air to move upwards. Consequently, this ascent enhances the thermal gradient between the Mediterranean Sea and the upper layers of the atmosphere. Sea

surface temperatures exceed 20 °C, thereby favoring strong evaporation, while temperatures above 5000 m above sea level are around -25 °C; this instability produces heavy showers, which, on certain occasions, contributes up to 80% of the total average annual precipitation in some of the meteorological stations in the analyzed area.

In turn, spring floods affect particularly the coastal stretch between the cities of Valencia and Alicante. The heavy rain conditions that usually affect these areas are characterized by a low-pressure center located over Cape Nao (i.e., northeast Alicante Province), whose movement is associated with a convergence line on its northeast flank, thereby directly impacting rainfall (Martínez Ibarra, 2012).

Finally, summer synoptic patterns affect more the municipalities located at the eastern SMC, and especially the city of Barcelona and its metropolitan area. This type of weather is a consequence of convection being enhanced by the overheating of the Iberian Peninsula. If a cold air mass is located aloft, instability increases, and clouds are formed, which may result in strong afternoon storms.

Most of the detected patterns are characterized by a low-pressure center that moves southward from the polar front until it is isolated aloft. This situation is especially recurrent in autumn, when two fundamental events coincide: the Mediterranean Sea exhibits high sea surface temperatures after the summer warming, while low-temperature air is found high in the troposphere. This atmospheric situation is known in Spanish by the acronym DANA, which stands for "isolated depression at high levels". When this occurs, a cold front clashes with warm air and produces heavy storms and torrential rainfall. In practice, DANA is a weather phenomenon quite similar to a cold drop, but its intensity and effects are much more devastating (Garcia-Ayllon and Radke, 2021).

This type of situation is especially evident among the highest incidence synoptic patterns (i.e., PSP1, PSP2, and PSP12); however, the location of DANA is determines the intensity of rainfall and the impact area, which lies at the leading edge of the depression, usually in the eastern and northeastern sectors of its periphery (Martin-Vide et al., 2021). In this regard, if DANA is located west of the Alboran Sea, heavy rainfall and floods are produced in the southern and central SMC; conversely, if it is located east of the Alboran Sea, intense precipitation occurs mainly in the central and northern SMC.

Monitoring DANA occurrences along the SMC is especially important for mitigating its effects on the population. Most catastrophic flood events almost always originate in a DANA. Several events of this type impacted severely the SMC: The September 1989 flood (Aragonés et al., 2016; Camarasa-Belmonte, 2016), which originated from a PSP1, affected 68 municipalities in seven different provinces, causing numerous fatalities and extensive damage in all economic sectors. The October 2000 flood was similar (Homar et al., 2002); on that occasion, the floods caused by a PSP8 affected 50 municipalities in five provinces, with substantial personal and material damage.

We note that DANA scenarios generally exhibit a characteristic synoptic configuration several days before the precipitation peak. This represents an opportunity to anticipate and prepare for intense rainfall, which is already being considered in early warning systems for floods (see Supplementary Material).

42% of the identified synoptic patterns exhibited a dipole, which indicates a spatial association between the incidence and severity of flood events in the southeastern and northeastern SMC. This dipole shows that floods associated with these synoptic patterns follow a path that first impacts the southwestern SMC in relation to an Atlantic low, and subsequently impacts the northeastern SMC due to a deepening of the low over the Mediterranean Sea. Nevertheless, synoptic patterns of great special incidence, as well as other secondary synoptic patterns, show great spatial coherence, as well as great incidence and intensity in the central and northeastern SMC. These synoptic patterns are related to a low-pressure area over the Mediterranean Sea and easterly or northeasterly surface winds.

4.2. Spatial variability of flood damage and implications for spatial planning

Geographical, social, and climate factors are essential for explaining high flood risk levels in the Mediterranean (Jodar-Abellan et al., 2019). In countries such as Greece (Bathrellos et al., 2016), Portugal (Motta et al., 2021), and Italy (Faccini et al., 2018), the zonification of these factors has been fundamental for appropriately limiting the flooding risk. Heterogeneity of the socioeconomic and environmental contexts hinders the definition of temporal trends in the flood behavior in large regions. In relation to this, Paprotny et al. (2018) detected in 37 European countries an increase in annually inundated areas and number of people affected since 1870. Nevertheless, there is a marked contrast between the trends observed in Mediterranean countries and countries elsewhere. Especially since 1950, in the Mediterranean countries there are significant declines in normalized deaths, persons affected, and monetary losses. These results are consistent with those of Gil-Guirado et al. (2019), who observed a decrease in flood severity in the SMC; however, the work of Paprotny et al. (2018) suggested that when the temporary behavior of flash floods in the Mediterranean is considered, the detected negative trends disappear. These different conclusions imply the need for determining the genesis of each flood; determining also the associated synoptic patterns is a necessary step in this regard.

Related to this, the trends in economic and human losses caused by floods seem to be closely related to the vulnerability of the SMC and its exposure to flood risk. Studies showed that the deficient urban planning in municipalities has led to increased institutional vulnerability (López-Martínez et al., 2017) and a concurrent exposure to flood danger (Pérez-Morales et al., 2016; Ribas et al., 2020). Because of these initial circumstances, it is very important to understand the types of damage associated with each synoptic pattern and when damage occurs. This is a key preliminary step in ensuring proper flood preparedness (Cherqui et al., 2015).

Regarding floods at municipal scale, we detected important hotspots where floods have increased recurrence. In this respect, it is in winter when municipalities west of the city of Malaga become an important hot spot. Nevertheless, the most important hot spots are the areas between the cities of Valencia and Alicante, as well as Barcelona and its metropolitan area. In the first case, the greatest flood impact occurs in spring, summer, and autumn; in the second case, flooding occurs primarily in autumn, but also in summer.

It is necessary to differentiate between the two possible causes to explain the seasonality and generation of hot spots. Each synoptic pattern recurs to a greater or lesser degree in each season of the year due to the meteorological causes indicated above. The origins of the low-pressure centers determine the temporal variability. While an Atlantic origin affects the study area during the cold seasons, mainly the southwestern SMC, a Mediterranean Sea origin or a deepening of its lows affects the study area during the warm seasons, especially the northeastern and eastern SMC.

The spatial variability and associated generation of hot spots may be due to the aforementioned synoptic conditions, higher population concentration, and economic activities in these hot spots. Regarding the first hypothesis, Romero et al. (1999a) highlighted the importance of mountainous coastal areas and their particular tendency to enhance torrential rainfall episodes. Similarly, Pastor et al. (2010) found that mountains close to the coast play a fundamental role in explaining the higher concentration of torrential precipitation in the area between Valencia and Alicante. Conversely, positive correlation between the size of cities and number of floods has been highlighted by López-Martínez et al. (2017) and Gil-Guirado et al. (2019), which invites researchers to continue delving deeper into the interrelationship between social and climatic variables within the context of flood-risk processes. In any case, appropriate planning of economic activities should consider the seasonal and spatial variability of each detected synoptic pattern. In this regard, the spatial differentiation of the type of damage produced by a flood can represent a significant improvement in flood prevention

systems, insofar as it allows the identification of where and at what time of year that economic sectors and damage types are most vulnerable to each synoptic pattern (Cortès et al., 2018). This can mean municipalities launching personalized monthly weather alerts with estimates of each synoptic pattern's damage probability based on the economic sector. Similar efforts have been made by some relevant European projects (Abily et al., 2020). Given the highly specialized commercial and tourism activities along the SMC (Ivars i Baidal et al., 2013), it is particularly important to create contingency plans for the tertiary sector. In the late summer months, tourism along the Mediterranean coast is still high and economic losses are amplified when these kinds of events occur, because tourists drastically reduce their period of stay and potential visitors tend to cancel their reservations. The latter is especially important for the coast of Barcelona, one of the world's top tourist destinations (Rico et al., 2019), which has a tourist model of high summer seasonality (Rodríguez-Algeciras et al., 2020), and represents added vulnerability to flooding.

In relation to temporal changes, the detected danger increase of some synoptic patterns should encourage local, regional, and national authorities to reconsider their adaptation strategies to floods. Regarding the reasons for these increases, we can neither confirm nor deny that these changes are due to the effects of climate change on rainfall behavior. Barriendos et al. (2019) were also not able to confirm or deny that these changes are due to increased exposure and vulnerability in the study area. However, the fact that the changes are limited to a few specific patterns suggests that, in addition to social causes, climatic causes are hidden behind this danger increase. The explanation probably lies within the evidence of global warming that occurred during the study period, when high pressures over the occidental part of Europe as well as Mediterranean fluxes intensified, especially during the warm seasons (Pörtner et al., 2019). Future research is needed to investigate the causes behind the spatiotemporal variability and trends observed in the behavior of floods according to synoptic patterns.

5. Conclusions

Twelve different synoptic patterns can statistically explain flood events along the SMC. The two dominant synoptic patterns are PSP1 and PSP8, which account for 60% of all events, while the rest of the synoptic patterns are of minor importance. Given this knowledge, authorities can adapt warning and prediction systems to the specific spatial differences and seasonality of each synoptic pattern. In five of the 12 patterns identified, we detected a dipole that indicates an association between the incidence and severity of flood events in the southeastern and northeastern SMC. Regarding seasonal differences, autumn is the season that has the largest number of flood events with the greatest intensity and extension (i.e., number of flood cases). Besides autumn, winter is the season with the greatest danger.

Regarding spatio-seasonal differences, we found that flood events associated with autumn patterns have a higher frequency and intensity in the eastern SMC, while winter patterns spatially affect the western sector.

At municipal scale, we detected important hot spots where floods have a greater recurrence, i.e., the coastline between the cities of Valencia and Alicante, as well as Barcelona and its metropolitan area.

Among the economic sectors, the tertiary sector is the most affected by floods along the SMC, followed by the primary and secondary sectors. Regarding the type of damage, roads and buildings are the most affected assets. Damage to the economic sector and damage types were both greater between August and November. According to the economic sector and type of damage, we detected synoptic patterns of varying degrees of impact. In general, PSP10 and PSP12 produced most of the damage, followed by PSP1 and PSP8; however, PSP12 needs special attention because fatalities during floods associated with this synoptic pattern occur in one out of every three floods.

Detected temporal trends regarding the behavior of some synoptic patterns indicate a troubling future. Conversely, we detected increases in both the number and extension (i.e., number of cases) of flood events. These statistically significant trends were detected in the most frequently occurring synoptic patterns (i.e., PSP1 and PSP8); however, the danger of synoptic patterns has overall increased (i.e., PSP3 and PSP11).

Finally, the results of this work should be incorporated into early warning systems that identify atmospheric patterns and their evolution; such practice would be instantaneously effective. Nevertheless, applying the proposed methodology to spatiotemporal databases has already proven to be of great value to policymakers, since the improved spatiotemporal identification of sensitive areas provides them with a tool for improving regional strategies.

Credit Author Statement.

The study conception and design has been coordinated by SG-G, with the support of DP, JCP and AP-M. SG-G, AP-M and FLM have carried out the data collection. SG-G has also written the main part of the paper. SG-G and JCP performed the statistical analysis. The interpretation of the results has been made by SG-G, with the support of the rest of the authors. All authors have coordinated the integration of the main part of the paper (tables, figures, texts and composition). SG-G and DP have coordinated the integration of texts between the different drafts. All authors have reviewed in depth the different drafts of the paper and the final version.

Declaration of competing interest

The authors have no conflicts of interest to declare.

Acknowledgements

This work has been supported by the Spanish Ministry of Science and Innovation/Agencia Estatal de Investigación and the European Regional Development Fund (ERDF/FEDER) through project ECCE (PID2020-115693RB-I00). SG-G acknowledges the support of the Spanish Ministry of Science, Innovation and Universities through "Juan de la Cierva-Incorporación" grant (IJCI-2016-29016).

Additionally, this work has been partially supported by the Spanish Ministry of Economy and Innovation (CGL2016-75996-R), the Spanish Ministry of Science, Innovation and Universities (CGL2013-43716-R; CGL2016-75475-R) and ICREA (ICREA Academia Program) and by the Spanish Ministry of Science and Innovation (PID2020-114576RB-I00).

We would also like to acknowledge the data and support provided by the Servei Meteorològic of Catalunya, the Institut Cartogràfic I Geològic of Catalunya and the Instituto Interuniversitario de Geografía of Alicante.

Appendix A. Supplementary data

Supplementary data to this article can be found online at https://doi.org/10.1016/j.scitotenv.2021.150777.

References

Abily, M., Gourbesville, P., De Carvalho Filho, E., Llort, X., Rebora, N., Sanchez, A., Sempere-Torres, D., 2020. Anywhere: enhancing emergency management and response to extreme weather and climate events. In: Gourbesville, P., Caignaert, G. (Eds.), Advances in Hydroinformatics. Springer Singapore, Singapore, pp. 29–37.

Aragonés, L., Pagán, J.I., López, M.P., García-Barba, J., 2016. The impacts of Segura River (Spain) channelization on the coastal seabed. Sci. Total Environ. 543, 493–504. https://doi.org/10.1016/j.scitotenv.2015.11.058.

Aran, M., Pena, J.C., Torà, M., 2011. Atmospheric circulation patterns associated with hail events in Lleida (Catalonia). Atmos. Res. 100, 428–438. https://doi.org/10.1016/j.atmosres.2010.10.029.

Armengot, R., Tamayo, J., Alcover Ronda, V., 1996. Centros de acción y flujo sinóptico en las precipitaciones intensas de la Comunidad Valenciana. III Simposio Nacional de Predicción Del Instituto Nacional de Meteorología. Instituto Nacional de Meteorología, Madrid, pp. 519–526.

Armon, M., Dente, E., Smith, J.A., Enzel, Y., Morin, E., 2018. Synoptic-scale control over modern rainfall and flood patterns in the levant drylands with implications for past climates. J. Hydrometeorol. 19, 1077–1096. https://doi.org/10.1175/JHM-D-18-0013.1.

Arrighi, C., Pregnolato, M., Dawson, R.J., Castelli, F., 2019. Preparedness against mobility disruption by floods. Sci. Total Environ. 654, 1010–1022. https://doi.org/10.1016/j.scitotenv.2018.11.191.

Barriendos, M., Gil-Guirado, S., Pino, D., Tuset, J., Pérez-Morales, A., Alberola, A., Costa, J., Balasch, J.C., Castelltort, X., Mazón, J., Ruiz-Bellet, J.L., 2019. Climatic and social factors behind the spanish Mediterranean flood event chronologies from documentary sources (14th–20th centuries). Glob. Planet. Chang. 182, 102997. https://doi.org/10.1016/j.gloplacha.2019.102997.

Bathrellos, G.D., Karymbalis, E., Skilodimou, H.D., Gaki-Papanastassiou, K., Baltas, E.A., 2016. Urban flood hazard assessment in the basin of Athens Metropolitan city, Greece. Environ. Earth Sci. 75, 319. https://doi.org/10.1007/s12665-015-5157-1.

Bathrellos, G.D., Skilodimou, H.D., Chousianitis, K., Youssef, A.M., Pradhan, B., 2017. Suitability estimation for urban development using multi-hazard assessment map. Sci. Total Environ. 575, 119–134. https://doi.org/10.1016/j.scitotenv.2016.10.025.

Brakenridge, G.R., 2014. Global Active Archive of Large Flood Events. [WWW Document]. URLDartmouth Flood Obs. Univ. Color (accessed 7.20.20 http://floodobservatory.colorado.edu/Archives/index.html.

Camarasa-Belmonte, A.M., 2016. Flash floods in Mediterranean ephemeral streams in Valencia region (Spain). J. Hydrol. 541, 99–115. https://doi.org/10.1016/j.jhydrol.2016.03.019.

Cattell, R.B., 1966. The scree test for the number of factors. Multivar. Behav. Res. 1, 245–276. https://doi.org/10.1207/s15327906mbr0102_10.

Cherqui, F., Belmeziti, A., Granger, D., Sourdril, A., Le Gauffre, P., 2015. Assessing urban potential flooding risk and identifying effective risk-reduction measures. Sci. Total Environ. 514, 418–425. https://doi.org/10.1016/j.scitotenv.2015.02.027.

Compo, G.P., Whitaker, J.S., Sardeshmukh, P.D., Matsui, N., Allan, R.J., Yin, X., Gleason, B.E., Vose, R.S., Rutledge, G., Bessemoulin, P., Brönnimann, S., Brunet, M., Crouthamel, R.I., Grant, A.N., Groisman, P.Y., Jones, P.D., Kruk, M.C., Kruger, A.C., Marshall, G.J., Maugeri, M., Mok, H.Y., Nordli, Ø., Ross, T.F., Trigo, R.M., Wang, X.L., Woodruff, S.D., Worley, S.J., 2011. The twentieth century reanalysis project. Q. J. R. Meteorol. Soc. 137, 1–28. https://doi.org/10.1002/qj.776.

Cortès, M., Turco, M., Llasat-Botija, M., Llasat, M.C., 2018. The relationship between precipitation and insurance data for floods in a Mediterranean region (northeast Spain). Nat. Hazards Earth Syst. Sci. 18, 857–868. https://doi.org/10.5194/nhess-18-857-2018.

CRED, EM-DAT, 2010. The OFDA/CRED international disaster database [WWW document]. URLUniv. Cathol. Louvain (accessed 7.25.20). https://www.emdat.be/.

Debatty, T., Michiardi, P., Mees, W., Thonnard, O., 2014. Determining the k in k-means with MapReduce. EDBT/ICDT Workshops, pp. 19–28.

Diab, R.D., Preston-Whyte, R.A., Washington, R., 1991. Distribution of rainfall by synoptic type over natal, South Africa. Int. J. Climatol. 11, 877–888. https://doi.org/10.1002/joc.3370110806.

Elsner, J.B., Drag, W.H., Last, J.K., 1989. Synoptic weather patterns associated with the Milwaukee, Wisconsin flash flood of 6 august 1986. Weather Forecast. 4, 537–554. https://doi.org/10.1175/1520-0434(1989)004<0537:SWPAWT>2.0.CO;2.

Esteban, P., Martin-Vide, J., Mases, M., 2006. Daily atmospheric circulation catalogue for western Europe using multivariate techniques. Int. J. Climatol. 26, 1501–1515. https://doi.org/10.1002/joc.1391.

Faccini, F., Luino, F., Paliaga, G., Sacchini, A., Turconi, L., de Jong, C., 2018. Role of rainfall intensity and urban sprawl in the 2014 flash flood in Genoa City, bisagno catchment (Liguria, Italy). Appl. Geogr. 98, 224–241. https://doi.org/10.1016/j.apgeog.2018.07.022.

Fiori, E., Ferraris, L., Molini, L., Siccardi, F., Kranzlmueller, D., Parodi, A., 2017. Triggering and evolution of a deep convective system in the Mediterranean Sea: modelling and observations at a very fine scale. Q. J. R. Meteorol. Soc. 143, 927–941. https://doi.org/10.1002/qj.2977.

Garcia-Ayllon, S., Radke, J., 2021. Geostatistical analysis of the spatial correlation between territorial anthropization and flooding vulnerability: application to the DANA phenomenon in a Mediterranean watershed. Appl. Sci. 11, 809. https://doi.org/10.3390/app11020809.

García-Valero, J.A., Montavez, J.P., Jerez, S., Gómez-Navarro, J.J., Lorente-Plazas, R., Jiménez-Guerrero, P., 2012. A seasonal study of the atmospheric dynamics over the Iberian Peninsula based on circulation types. Theor. Appl. Climatol. 110, 291–310. https://doi.org/10.1007/s00704-012-0623-0.

Giannaros, C., Kotroni, V., Lagouvardos, K., Oikonomou, C., Haralambous, H., Papagiannaki, K., 2020. Hydrometeorological and socio-economic impact assessment of stream flooding in Southeast Mediterranean: the case of Rafina catchment (Attica, Greece). Water 12, 2426. https://doi.org/10.3390/w12092426.

Gilabert, J., Llasat, M.C., 2018. Circulation weather types associated with extreme flood events in northwestern Mediterranean. Int. J. Climatol. 38, 1864–1876. https://doi.org/10.1002/joc.5301.

Gil-Guirado, S., Espín-Sánchez, J.-A., Del Rosario Prieto, M., 2016. Can we learn from the past? Four hundred years of changes in adaptation to floods and droughts. Measuring the vulnerability in two Hispanic cities. Clim. Chang. 139, 183–200. https://doi.org/10.1007/s10584-016-1768-0.

Gil-Guirado, S., Pérez-Morales, A., Lopez-Martinez, F., 2019. SMC-flood database: a high-resolution press database on flood cases for the spanish Mediterranean coast (1960–2015). Nat. Hazards Earth Syst. Sci. 19, 1955–1971. https://doi.org/10.5194/nhess-19-1955-2019.

Gochis, D., Schumacher, R., Friedrich, K., Doesken, N., Kelsch, M., Sun, J., Ikeda, K., Lindsey, D., Wood, A., Dolan, B., Matrosov, S., Newman, A., Mahoney, K., Rutledge, S., Johnson, R., Kucera, P., Kennedy, P., Sempere-Torres, D., Steiner, M., Roberts, R., Wilson, J., Yu, W., Chandrasekar, V., Rasmussen, R., Anderson, A., Brown, B., 2015. The great Colorado flood of september 2013. Bull. Am. Meteorol. Soc. 96, 1461–1487. https://doi.org/10.1175/BAMS-D-13-00241.1.

Grimalt-Gelabert, M., Alomar-Garau, G., Martin-Vide, J., 2021. Synoptic causes of torrential rainfall in the Balearic Islands (1941–2010). Atmosphere 12, 1035. https://doi.org/10.3390/atmos12081035.

Hirsch, R.M., Slack, J.R., 1984. A nonparametric trend test for seasonal data with serial dependence. Water Resour. Res. 20, 727–732. https://doi.org/10.1029/WR020i006p00727.

Homar, V., Romero, R., Ramis, C., Alonso, S., 2002. Numerical study of the october 2000 torrential precipitation event over eastern Spain: analysis of the synoptic-scale stationarity. Ann. Geophys. 20, 2047–2066. https://doi.org/10.5194/angeo-20-2047-2002.

Hurrell, J.W., 1995. Decadal trends in the North Atlantic Oscillation: regional temperatures and precipitation. Science (80-.) 269, 676–679. https://doi.org/10.1126/science.269.5224.676.

Huth, R., 1996a. An intercomparison of computer-assisted circulation classification methods. Int. J. Climatol. 16, 893–922. https://doi.org/10.1002/(SICI)1097-0088(199608)16:8<893::AID-JOC51>3.0.CO;2-Q.

Huth, R., 1996b. Properties of the circulation classification scheme based on the rotated principal component analysis. Meteorog. Atmos. Phys. 59, 217–233. https://doi.org/10.1007/BF01030145.

Huth, R., Beck, C., Philipp, A., Demuzere, M., Ustrnul, Z., Cahynová, M., Kyselý, J., Tveito, O.E., 2008. Classifications of atmospheric circulation patterns: recent advances and applications. Ann. N. Y. Acad. Sci. 1146, 105–152. https://doi.org/10.1196/annals.1446.019.

Ivars i Baidal, J.A., Rodríguez Sánchez, I., Vera Rebollo, J.F., 2013. The evolution of mass tourism destinations: new approaches beyond deterministic models in Benidorm (Spain). Tour. Manag. 34, 184–195. https://doi.org/10.1016/j.tourman.2012.04.009.

Jodar-Abellan, A., Valdes-Abellan, J., Pla, C., Gomariz-Castillo, F., 2019. Impact of land use changes on flash flood prediction using a sub-daily SWAT model in five Mediterranean ungauged watersheds (SE Spain). Sci. Total Environ. 657, 1578–1591. https://doi.org/10.1016/j.scitotenv.2018.12.034.

Kahana, R., Ziv, B., Enzel, Y., Dayan, U., 2002. Synoptic climatology of major floods in the Negev Desert, Israel. Int. J. Climatol. 22, 867–882. https://doi.org/10.1002/joc.766.

Kalnay, E., Kanamitsu, M., Kistler, R., Collins, W., Deaven, D., Gandin, L., Iredell, M., Saha, S., White, G., Woollen, J., Zhu, Y., Leetmaa, A., Reynolds, R., Chelliah, M., Ebisuzaki, W., Higgins, W., Janowiak, J., Mo, K.C., Ropelewski, C., Wang, J., Jenne, R., Joseph, D., 1996. The NCEP/NCAR 40-year reanalysis project. Bull. Am. Meteorol. Soc. 77, 437–471. https://doi.org/10.1175/1520-0477(1996)077<0437:TNYRP>2.0.CO;2.

Kisi, O., Ay, M., 2014. Comparison of Mann–Kendall and innovative trend method for water quality parameters of the Kizilirmak River, Turkey. J. Hydrol. 513, 362–375. https://doi.org/10.1016/j.jhydrol.2014.03.005.

Kourgialas, N.N., Karatzas, G.P., 2017. A national scale flood hazard mapping methodology: the case of Greece – protection and adaptation policy approaches. Sci. Total Environ. 601–602, 441–452. https://doi.org/10.1016/j.scitotenv.2017.05.197.

Lira, C., Lousada, M., Falcão, A.P., Gonçalves, A.B., Heleno, S., Matias, M., Pereira, M.J., Pina, P., Sousa, A.J., Oliveira, R., Almeida, A.B., 2013. The 20 february 2010 Madeira Island flash-floods: VHR satellite imagery processing in support of landslide inventory and sediment budget assessment. Nat. Hazards Earth Syst. Sci. 13, 709–719. https://doi.org/10.5194/nhess-13-709-2013.

Llasat, M.C., Barriendos, M., Barrera, A., Rigo, T., 2005. Floods in Catalonia (NE Spain) since the 14th century. climatological and meteorological aspects from historical documentary sources and old instrumental records. J. Hydrol. 313, 32–47. https://doi.org/10.1016/j.jhydrol.2005.02.004.

López-Martínez, F., Gil-Guirado, S., Pérez-Morales, A., 2017. Who can you trust? Implications of institutional vulnerability in flood exposure along the spanish Mediterranean coast. Environ. Sci. Policy 76, 29–39. https://doi.org/10.1016/j.envsci.2017.06.004.

Lynch, S.L., Schumacher, R.S., 2014. Ensemble-based analysis of the may 2010 extreme rainfall in Tennessee and Kentucky. Mon. Weather Rev. 142, 222–239. https://doi.org/10.1175/MWR-D-13-00020.1.

Maddox, R.A., Chappell, C.F., Hoxit, L.R., 1979. Synoptic and meso-α scale aspects of flash flood Events1. Bull. Am. Meteorol. Soc. 60, 115–123. https://doi.org/10.1175/1520-0477-60.2.115.

Maddox, R.A., McCollum, D.M., Howard, K.W., 1995. Large-scale patterns associated with severe summertime thunderstorms over Central Arizona, weather and forecasting. Am. Meteorol. Soc. https://doi.org/10.1175/1520-0434(1995)010<0763:LSPAWS>2.0.CO;2.

Marco Ortega, V., Estrela, M.J., Miró, J.J., Gómez, Montávez, Pedro, Juan, 2018. Precipitación intensa en la región de Murcia. Distribución espacial y relación con la circulación sinóptica (1980-2000). El Clima: Aire, Agua, Tierra y Fuego. Agencia Estatal de Meteorología, Madrid, pp. 103–113.

Martínez Ibarra, E., 2012. A geographical approach to post-flood analysis: the extreme flood event of 12 october 2007 in calpe (Spain). Appl. Geogr. 32, 490–500. https://doi.org/10.1016/j.apgeog.2011.06.003.

Martin-Vide, J., Sanchez-Lorenzo, A., Lopez-Bustins, J.A., Cordobilla, M.J., Garcia-Manuel, A., Raso, J.M., 2008. Torrential rainfall in northeast of the Iberian Peninsula: synoptic patterns and WeMO influence. Adv. Sci. Res. 2, 99–105. https://doi.org/10.5194/asr-2-99-2008.

Martin-Vide, J., Moreno-Garcia, M.C., Lopez-Bustins, J.A., 2021. Synoptic causes of torrential rainfall in South-Eastern Spain (1941–2017). Geogr. Res. Lett. 1–19. https://doi.org/10.18172/cig.4696.

Michailidou, C., Maheras, P., Arseni-Papadimititriou, A., Kolyva-Machera, F., Anagnostopoulou, C., 2009. A study of weather types at Athens and Thessaloniki and their relationship to circulation types for the cold-wet period, part II: discriminant analysis. Theor. Appl. Climatol. 97, 179–194. https://doi.org/10.1007/s00704-008-0058-9.

Milrad, S.M., Gyakum, J.R., Atallah, E.H., 2015. A meteorological analysis of the 2013 Alberta flood: antecedent large-scale flow pattern and synoptic-dynamic characteristics. Mon. Weather Rev. 143, 2817–2841. https://doi.org/10.1175/MWR-D-14-00236.1.

Monge, J.J., McDonald, N., McDonald, G.W., 2022. A review of graphical methods to map the natural hazard-to-wellbeing risk chain in a socio-ecological system. Sci. Total Environ. 803, 149947. https://doi.org/10.1016/j.scitotenv.2021.149947.

Motta, M., de Castro Neto, M., Sarmento, P., 2021. A mixed approach for urban flood prediction using machine learning and GIS. Int. J. Disaster Risk Reduct. 56, 102154. https://doi.org/10.1016/j.ijdrr.2021.102154.

Munich Re, 2015. NatCat SERVICE loss database for natural catastrophes worldwide. [WWW document]. URL http://www.munichre.com/en/reinsurance/business/non-life/georisks/natcatservice/default.aspx (accessed 7.20.20).

Niedźwiedź, T., Łupikasza, E., Pińskwar, I., Kundzewicz, Z.W., Stoffel, M., Małarzewski, Ł., 2015. Variability of high rainfalls and related synoptic situations causing heavy floods at the northern foothills of the Tatra Mountains. Theor. Appl. Climatol. 119, 273–284. https://doi.org/10.1007/s00704-014-1108-0.

Paprotny, D., Sebastian, A., Morales-Nápoles, O., Jonkman, S.N., 2018. Trends in flood losses in Europe over the past 150 years. Nat. Commun. 9, 1985. https://doi.org/10.1038/s41467-018-04253-1.

Pastor, F., Gómez, I., Estrela, M.J., 2010. Numerical study of the october 2007 flash flood in the Valencia region (Eastern Spain): the role of orography. Nat. Hazards Earth Syst. Sci. 10, 1331–1345. https://doi.org/10.5194/nhess-10-1331-2010.

Peleg, N., Morin, E., 2012. Convective rain cells: radar-derived spatiotemporal characteristics and synoptic patterns over the eastern Mediterranean. J. Geophys. Res. Atmos. 117. https://doi.org/10.1029/2011JD017353.

Peña, J.C., Aran, M., Cunillera, J., Amaro, J., 2011. Atmospheric circulation patterns associated with strong wind events in Catalonia. Nat. Hazards Earth Syst. Sci. 11, 145–155. https://doi.org/10.5194/nhess-11-145-2011.

Peña, J.C., Aran, M., Pérez-Zanón, N., Casas-Castillo, M.C., Rodríguez-Solà, R., Redaño, A., 2015. Análisis de las situaciones sinópticas correspondientes a episodios de lluvia severa en Barcelona. XXXV Reunión Bienal de La Real Sociedad Española de Física. Libro de Resúmenes. Real Sociedad Española de Física (RSEF), Madrid, pp. 450–451. https://doi.org/10.1007/s00704-003-0003-xD.

Pérez-Morales, A., Gil-Guirado, S., Olcina, J., 2016. La información catastral Como herramienta Para el análisis de la exposición al peligro de inundaciones en el Litoral mediterráneo español. Eure 42, 231–256. https://doi.org/10.4067/s0250-71612016000300010.

Pérez-Morales, A., Gil-Guirado, S., Olcina-Cantos, J., 2018. Housing bubbles and the increase of flood exposure. failures in flood risk management on the spanish southeastern coast (1975–2013). J. Flood Risk Manag. 11, S302–S313. https://doi.org/10.1111/jfr3.12207.

Pino, D., Ruiz-Bellet, J.L., Carles, J., Romero-León, L., Tuset, J., Barriendos, M., Mazon, J., Castelltort, X., 2016. Meteorological and hydrological analysis of major floods in NE Iberian Peninsula. J. Hydrol. 541, 63–89. https://doi.org/10.1016/j.jhydrol.2016.02.008.

Pohlert, T., 2016. Package 'trend'. Non-Parametric Trend Tests and Change-Point Detectione.

Pörtner, H.-O., Roberts, D.C., Masson-Delmotte, V., Zhai, P., Tignor, M., Poloczanska, E., Mintenbeck, K., Alegría, A., Nicolai, M., Okem, A., Petzold, J., Rama, B., Weyer, N.M., 2019. IPCC Special Report on the Ocean and Cryosphere in a Changing Climate.

QGIS Development Team, 2016. QGIS Geographic Information System.

R Core Team, 2019. R: A Language and Environment for Statistical Computing.

Ribas, A., Olcina, J., Sauri, D., 2020. More exposed but also more vulnerable? Climate change, high intensity precipitation events and flooding in Mediterranean Spain. Disaster Prev Manag 29, 229–248. https://doi.org/10.1108/DPM-05-2019-0149.

Richman, M.B., 1986. Rotation of principal components. J. Climatol. 6, 293–335. https://doi.org/10.1002/joc.3370060305.

Rico, A., Martínez-Blanco, J., Montlleó, M., Rodríguez, G., Tavares, N., Arias, A., Oliver-Solà, J., 2019. Carbon footprint of tourism in Barcelona. Tour. Manag. 70, 491–504. https://doi.org/10.1016/j.tourman.2018.09.012.

Rodríguez-Algeciras, J., Rodríguez-Algeciras, A., Chaos-Yeras, M., Matzarakis, A., 2020. Tourism-related climate information for adjusted and responsible planning in the tourism industry in Barcelona, Spain. Theor. Appl. Climatol. 142, 1003–1014. https://doi.org/10.1007/s00704-020-03341-x.

Romero, R., Ramis, C., Guijarro, J.A., 1999a. Daily rainfall patterns in the spanish Mediterranean area: an objective classification. Int. J. Climatol. 19, 95–112. https://doi.org/10.1002/(SICI)1097-0088(199901)19:1<95::AID-JOC344>3.0.CO;2-S.

Romero, R., Sumner, G., Ramis, C., Genovés, A., 1999b. A classification of the atmospheric circulation patterns producing significant daily rainfall in the spanish Mediterranean area. Int. J. Climatol. 19, 765–785. https://doi.org/10.1002/(SICI)1097-0088(19990615)19:7<765::AID-JOC388>3.0.CO;2-T.

Seager, R., Liu, H., Kushnir, Y., Osborn, T.J., Simpson, I.R., Kelley, C.R., Nakamura, J., 2020. Mechanisms of winter precipitation variability in the european-Mediterranean region associated with the North Atlantic oscillation. J. Clim. 33, 7179–7196. https://doi.org/10.1175/JCLI-D-20-0011.1.

Sen, P.K., 1968. Estimates of the regression coefficient based on Kendall's tau. J. Am. Stat. Assoc. 63, 1379–1389. https://doi.org/10.1080/01621459.1968.10480934.

Sioutas, M.V., Flocas, H.A., 2003. Hailstorms in northern Greece: synoptic patterns and thermodynamic environment. Theor. Appl. Climatol. 75, 189–202. https://doi.org/10.1007/s00704-003-0734-8.

Stucki, P., Rickli, R., Brönnimann, S., Martius, O., Wanner, H., Grebner, D., Luterbacher, J., 2012. Weather patterns and hydro-climatological precursors of extreme floods in Switzerland since 1868. Meteorol. Z. 21, 531–550. https://doi.org/10.1127/0941-2948/2012/368.

Swiss-Re, 2017. Sigma natural catastrophes and man-made disasters. [WWW document]. URL http://institute.swissre.com/research/overview/sigma/ (accessed 6.15.20).

Thorndike, R.L., 1953. Who belongs in the family? Psychometrika 18, 267–276. https://doi.org/10.1007/BF02289263.

Tibshirani, R., Walther, G., Hastie, T., 2001. Estimating the number of clusters in a data set via the gap statistic. J. R. Stat. Soc. Ser. B Stat Methodol. 63, 411–423. https://doi.org/10.1111/1467-9868.00293.

Trigo, R.M., Varino, F., Ramos, A.M., Valente, M.A., ZÃazere, J.L., Vaquero, J.M., Gouveia, C.M., Russo, A., 2014. The record precipitation and flood event in Iberia in December 1876: description and synoptic analysis. Front. Earth Sci., 2. https://doi.org/10.3389/feart.2014.00003.

Zhang, Y., Moges, S., Block, P., 2016. Optimal cluster analysis for objective regionalization of seasonal precipitation in regions of high spatial-temporal variability: application to Western Ethiopia. J. Clim. 29, 3697–3717. https://doi.org/10.1175/JCLI-D-15-0582.1.